Design of a Single-DOF Immersive Rehabilitation Device for Clustered Upper Limb Motion

Article *in* Journal of Mechanisms and Robotics · February 2021

DOI: 10.1115/1.4050150

Ping Zhao
Hefei University of Technology

Xueting Deng
Stony Brook University

Haodong Chen
University of Maryland, College Park

Ping Zhao[1]
School of Mechanical Engineering,
Hefei University of Technology,
Hefei, Anhui 230009, China
e-mail: ping.zhao@hfut.edu.cn

Yating Zhang
School of Mechanical Engineering,
Hefei University of Technology,
Hefei, Anhui 230009, China
e-mail: yting.zhang@qq.com

Haiwei Guan
School of Mechanical Engineering,
Hefei University of Technology,
Hefei, Anhui 230009, China
e-mail: philosopher1897@foxmail.com

Xueting Deng
Department of Mechanical Engineering,
Stony Brook University,
Stony Brook, NY 11794
e-mail: xueting.deng@stonybrook.edu

Haodong Chen
Department of Mechanical and Aerospace Engineering,
Missouri University of Science and Technology,
Rolla, MO 65301
e-mail: h.chen@mst.edu

Design of a Single-Degree-of-Freedom Immersive Rehabilitation Device for Clustered Upper-Limb Motion

Mechanical devices such as robots are widely adopted for limb rehabilitation. Due to the variety of human body parameters, the rehabilitation motion for different patients usually has its individual pattern; hence, we adopt clustering-based machine learning technique to find a limited number of motion patterns for upper-limb rehabilitation, so that they could represent the large amount of those from people who have various body parameters. By using the regression motion of the clustering result as the target, in this article, we seek to apply kinematic mapping-based motion synthesis framework to design a 1-degree-of-freedom (DOF) mechanism, such that it could lead the patients' upper limb through the target motion. Also, considering rehab training generally involves a large amount of repetition on a daily basis, this article has developed a rehab system with UNITY3D based on virtual reality (VR). The proposed device and system could provide an immersive experience to the users, as well as the rehab motion data to the administrative staff for evaluation of users' status. The construction of the integrated system and the experimental trial of the prototype are presented at the end of this article. [DOI: 10.1115/1.4050150]

Keywords: *mechanism design, mechanism synthesis, medical robotics*

1 Introduction

In recent years, mechanical assisting devices such as robots have been recognized as one of the most significant developments in emerging industries [1,2]. Especially in those fields that require a large amount of human resources, the adoption of robots and other intelligent devices could drastically reduce the cost and improve the efficiency. Rehabilitation of patients of disabilities, after-strokes, etc. is one of the novel medical fields that has been recently started to apply the intelligent devices so as to provide effective training for the patients and also to reduce the cost of clinical caring staff. This article focuses on the development of an upper-limb rehabilitation mechanism, i.e., an automatic device for assisting patients with upper-limb dysfunction to complete the rehabilitation training and provide feedback information for rehabilitation physicians and patients. Currently, the structural design of upper-limb rehabilitation devices and robots are mainly accomplished with end traction mechanism and exoskeleton mechanism [3]. The former basically takes linkages or serial robots as the essential motion executer and realizes the repeated rehabilitation training by supporting and guiding the end of the patient's upper limb. For example, Holt et al. designed a dual-arm robot called iPAM [4], and a 2-degree-of-freedom (DOF) upper-limb rehabilitation robot named UECM was developed by Zhang et al. [5]. The exoskeletons, on the other hand, usually have a structure that accommodates with human body and transmit forces to the limb to assist rehabilitation training. Examples of this type of rehabilitation mechanisms include the 7-DOF exoskeleton powered arm CADEN-7, which was designed by Perry et al. [6] and a 3-DOF EMUL rehabilitation robot that was developed by Haraguchi et al. from Osaka University [7]. Considering the cost of these multi-DOF rehab devices is usually quite expensive, designers also proposed a series of 1-DOF rehab mechanisms for specified tasks. Naghavi and Mahjoob [8] proposed an active 1-DOF mechanism for knee rehabilitation. Franci et al. [9] designed a parallel mechanism for modeling passive motion at the human tibiotalar joint. Our group [10] also proposed a cam-linkage mechanism for lower-limb rehabilitation with kinematic mapping-based motion synthesis approach.

Since human body parameters vary among each individual, apparently the suitable rehabilitation motion for different patients should also have different patterns. If 1-DOF rehabilitation mechanisms are adopted for its simpler structure and lower cost, then a group of different mechanisms need to be prepared to adjust different users since 1-DOF mechanisms can only generate one specified motion. Conversely, to address such issues, most of the current multi-DOF limb rehabilitation mechanisms are controlled and programmed to produce training trajectories in different scales to reflect the limb length. Yet, body parameters such as height and weight also affect the trajectories, but they are usually not considered. It would also be unpractical to customize a different motion or mechanism for each user individually. Therefore, in our previous study [11], we adopted several clustering algorithms of unsupervised machine learning to find three motion patterns for upper-limb rehabilitation, so that they could represent the large amount of those from people who have various body parameters. Using the regression motion of the three clusters as the task motion, in this article, we are seeking to design a one-DOF mechanism, such that it could lead the patients' upper limb through the task motion.

It is known that designing a mechanism to lead a rigid-body through a sequence of given poses is a classic kinematic task called motion synthesis [12,13]. In those designs, linkage mechanisms, i.e., mechanisms that contains only planar low pairs, are generally the goal that researchers focusing on due to its simpleness to analyze and convenience to manufacture. This problem is usually solved by numerical optimization algorithms. In our previous work [14–16], we have also presented a framework of an efficient

[1]Corresponding author.

Contributed by the Mechanisms and Robotics Committee of ASME for publication in the JOURNAL OF MECHANISMS AND ROBOTICS. Manuscript received September 26, 2020; final manuscript received February 4, 2021; published online March 12, 2021. Assoc. Editor: Pinhas Ben-Tzvi.

algorithm for motion approximation of linkage mechanisms. This approach is based on the kinematic mapping theory that was first explored by Bottema and Roth [17] for application in planar linkage design and then developed by McCarthy [18] and Ravani and Roth [19]. This theory was further adopted and extended by several other researchers [20–24]. Based on our kinematic mapping-based motion synthesis framework, a simple four-bar linkage mechanism is proposed to realize the task motion in this article, which is simpler, lower cost, and easier to control compared with the multi-DOF limb rehab devices.

According to the limb rehabilitation requirements, the training process usually involves a large amount of repetition of rehab motion in daily basis, which could be quite tedious for most patients [25]. Therefore, in this article, we are adopting virtual reality (VR) technique to create an immersive rehabilitation training mode to help the patients to improve their training experiences. Virtual reality refers to a highly realistic computer-simulated environment in terms of sight, hearing, touch, etc. Users can interact with this environment to produce an immersive experience. Users can observe items in the three-dimensional space in a timely and unlimited manner. They can also interact with items in the virtual reality with the help of tools. When the user moves and/or manipulates an assisting tool, the computer can immediately perform complex calculations to accurately produce a sense of presence, controlling intelligent hardware to give users feedback on multiple channels to produce real-time changes in perception. In recent years, the use of virtual reality technology in the areas of rehabilitation and therapy continues to grow [26–29], with encouraging results being reported for applications that address human physical, cognitive, and psychological functioning. This article incorporates VR technique to the upper-limb rehabilitation device and designs an immersive rehab system as well as a displays user interface for the caring staff to better support the patients' training process.

The organization of this article is as follows: Sec. 2 presents how the upper-limb rehab motion trajectory data are acquired and clustered to generate the task motion. Then, Sec. 3 briefly introduces our kinematic mapping-based framework, and based on that, a four-bar linkage is designed to serve as the rehab motion executer, with which a simple one-DOF device is developed to generate the rehab motion. In Sec. 4, virtual reality technique is adopted to create an immersive rehabilitation training mode, and a patient user interface is designed with Unity3D. Then, Sec. 5 shows the integration of the whole system with two-mode (passive and active) rehabilitation strategy and presents a system prototype as well as experiment results of human trial.

2 Acquisition of Upper-Limb Rehabilitation Motion Trajectory Data

The upper-limb rehabilitation training motion we are trying to implement is a boating movement as shown in Fig. 1(*a*).Our data acquisition environment is a high-precision labeled motion capture system named cortex (Figs. 1(*b*) and (*c*)), in which eight cameras are set around the subject to record data and trajectory extraction. During the data acquisition process, the real-time trajectories of 25 small balls that are attached to each joint of the subject are acquired. The spatial location information of the specified three points *S*, *E*, and *W* on the left arm is obtained, where the three points S, E, and W represent, respectively, three small balls fixed to the shoulder joint, the elbow joint, and the wrist joint. A total number of 47 healthy subjects have participated in the data collecting process, who wear the experiment equipment for the motion capture. After learning from the demonstration video of rehabilitation training motion, the subjects accomplished the specified boating movement for upper-limb rehabilitation training in the environment of trajectory acquisition. Debugging and coordinate calibration of the experiment equipment were also completed before operating the device to record the trajectory data.

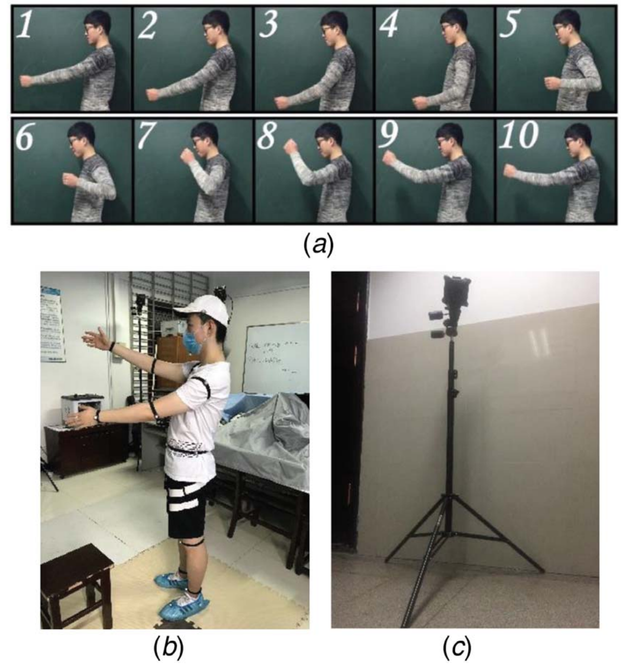

Fig. 1 The demonstration of (*a*) upper-limb rehabilitation motion and (*b*) and (*c*) the trajectory capture device

After capturing the raw data of the boating motion from the subjects, these data sets are first preinterpolated and processed to reduce the noises. To improve the performance of clustering, it is a commonly adopted strategy to expand the database by separating one original set of data to multiple sets. In our case, to expand the database, we uniformly sample 24 frames in a complete motion of about 120 frames. Thus, the database is now expanded to 94 sets.

Due to the variety of human body parameters, in our previous study [11], we have adopted clustering-based machine learning technique to find a limited number of motion patterns for upper-limb rehabilitation, so that they could represent the large amount of those from people who have various body parameters. Spectral clustering (SC) method was chosen for its performance, and as shown in Fig. 2, three clusters of motion patterns (blue/dot, green/circle, and red/star) are formed. After regression of each cluster, three types of motion for upper-limb rehabilitation are constructed, which could serve as the task motion for the design of rehabilitation mechanisms.

To actually obtain the pattern and trend for each cluster of rehabilitation motion, we still take the three points' (shoulder joints S, elbow joints E, and wrist joints W) spatial coordinates of each cluster generated by spectral clustering algorithm and conduct a regression for each cluster of motion. Figure 3 shows the regression result of the S, E, and W joints' spatial trajectory of the three type of clusters. It could be noticed that the shoulder joint trajectory is a small closed curve in all types of motion, which is generally treated as a fixed sphere joint in practical design cases.

3 Kinematic Mapping-Based Mechanism Synthesis for Task Motion

Now, to design a 1-DOF upper-limb rehabilitation device, the blue cluster in Fig. 2 is taken in this article as the task motion for it represents the most data sets. The original motion in Ref. [11] contains 24 poses from the 24 frames, and 4 additional poses are interpolated between the starting and ending pose so as to form a smoother closed loop motion. The coordinate data of these 28 poses are listed in the supplement files. The aim is to determine a mechanism such that it could lead its manipulator through the boating

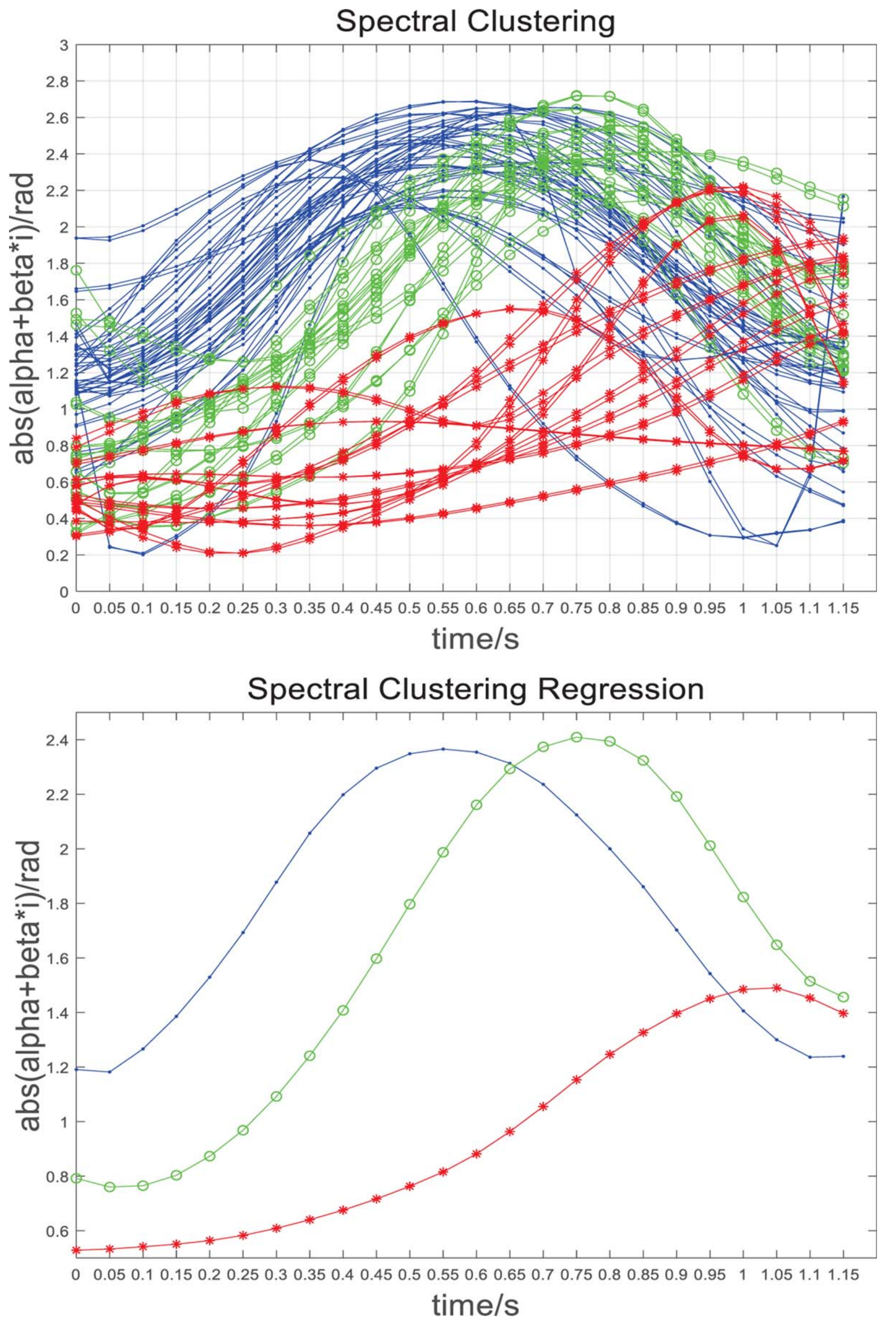

Fig. 2 The clustering (above) as well as regression (below) of 94 sets of rehabilitation motion data using the SC method. $\alpha+\beta i$ is defined in Ref. [11], so as to reflect the trend and pattern of the upper-limb poses during the boating rehabilitation motion

rehabilitation motion. It could be noticed in Fig. 3 that the elbow and the wrist trajectories of the blue spatial motion could be approximately viewed as in the same plane. Thus, in this section, we approximate the spatial forearm motion in Fig. 3 to a planar one and seek to use 1-DOF mechanisms to lead through it.

First, the 28 discretized spatial forearm poses of this motion are fitted to a plane. As shown in Fig. 4, the expression of the fitting plane is expressed as follows:

$$-0.8687a + 0.4736b - 0.1449c - 65.9624 = 0 \tag{1}$$

The two light curves of Fig. 4 are the projection of the two trajectories in the left of Fig. 3. They are plotted as two planar curves in the right figure, and connecting each pair of corresponding elbow trajectory point and wrist trajectory point yields 28 line segments with location and angle, which are identified as 28 task planar poses to be lead through. Next, we use our kinematic mapping-based planar motion synthesis framework [14,15] to design a planar one-DOF mechanism that approximates this rehabilitation motion. Considering a planar moving rigid-body represented with a quaternion $\mathbf{Z} = (Z_1, Z_2, Z_3, Z_4)$ [17], if it is capable to be led through by the moving frame of a planar dyad (two-bar linkage), then a unified quadratic equation needs to be satisfied:

$$\begin{aligned} &p_1(Z_1^2 + Z_2^2) + p_2(Z_1Z_3 - Z_2Z_4) + p_3(Z_2Z_3 + Z_1Z_4) \\ &\quad + p_4(Z_1Z_3 + Z_2Z_4) + p_5(Z_2Z_3 - Z_1Z_4) + p_6Z_3Z_4 \\ &\quad + p_7(Z_3^2 - Z_4^2) + p_8(Z_3^2 + Z_4^2) = 0 \end{aligned} \tag{2}$$

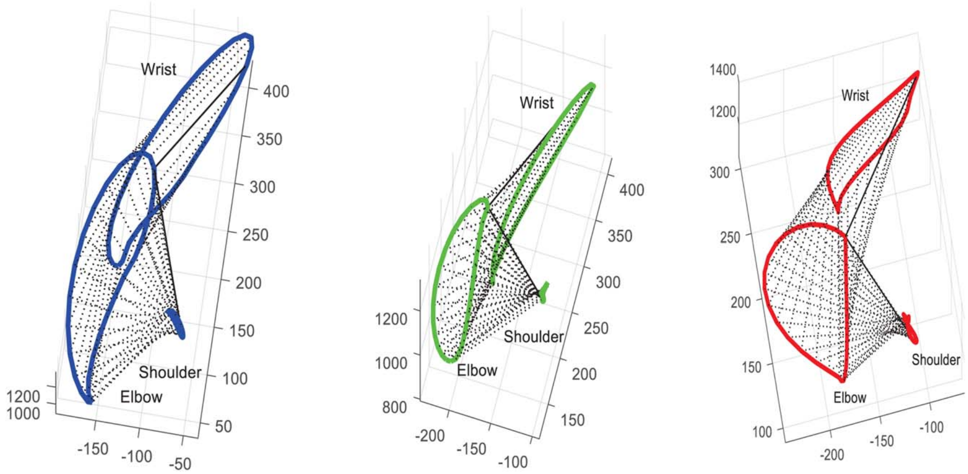

Fig. 3 Upper-limb rehabilitation joint trajectories in Fig. 2: blue cluster (left), green cluster (middle), and red cluster (right) (Color version online.)

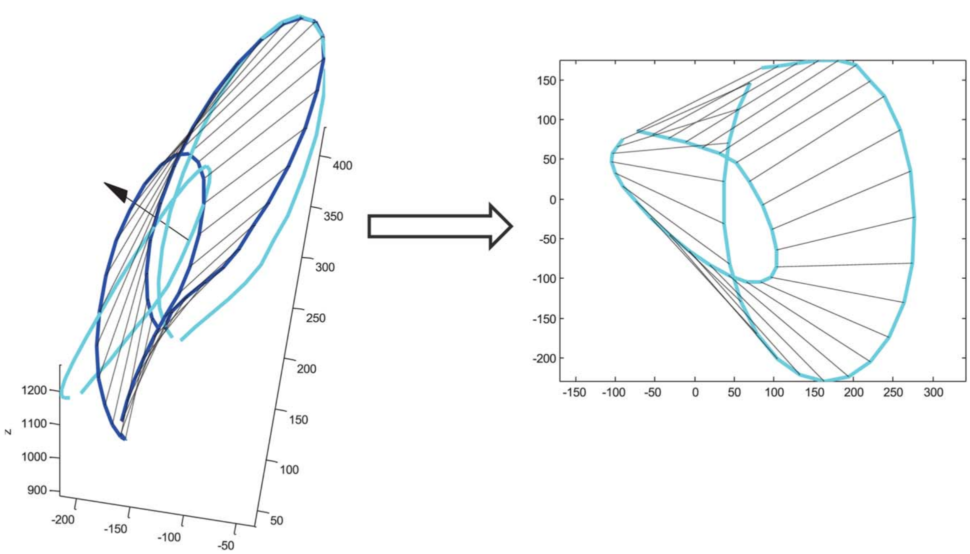

Fig. 4 The spatial forearm motion (including both the elbow and wrist trajectories) is projected to a plane, and this planar approximated motion on the right figure is the to-be-realized task motion

with two unified additional constraints on coefficients p_1 through p_7:

$$
\begin{aligned}
p_1p_6 + p_2p_5 - p_3p_4 &= 0 \\
2p_1p_7 - p_2p_4 - p_3p_5 &= 0
\end{aligned} \tag{3}
$$

where coefficient vector $\mathbf{p} = (p_1, p_2, \ldots p_8)$ is constructed with only the parameters of the planar dyad, including its fixed frame and moving frame parameters. In this way, the prescribed task information ($\mathbf{Z}$) and the to-be-determined information ($\mathbf{p}$) are separated. The aforementioned conditions apply to all three common types of planar dyads: RR, PR, or RP. This system could be solved with null space analysis technique [15], which yields a group of resulting vector $\mathbf{p}$. Furthermore, by investigating the value of $\mathbf{p}$, we can determine the type and dimensions of the resulting dyads. Applying this kinematic synthesis method to the 28 task poses in Fig. 4, several planar dyads are obtained that could lead through this upper-limb rehabilitation motion. The parameters of these dyads are listed in Table 1. The first two dyads are taken from Table 1 and combined them to form a one-DOF four-bar linkage. In Fig. 5, we show the coupler motion that generated by this four-bar crank-rocker linkage. It could be seen that the trajectory (light blue) leads through the 28 prescribed poses (black). Compared with multi-DOF linkages, upper-limb rehabilitation device equipped with such a one-DOF mechanism could still approximately realize the rehabilitation task, while maintaining a simpler structure and control mode as well as a much lower cost.

Now that the essential motion executer (i.e., the four-bar linkage synthesized to lead through the rehabilitation motion) has been given, we seek to design a one-DOF upper-limb rehab device with this motion executer. Considering the health condition of the patient, the device is designed to adopt sitting-position rehabilitation training mode. Aside of the motion executer, an adjustable

Table 1 Dimensions of the four planar dyads that could lead through the planar motion poses in Fig. 4

	Fixed pivot	Moving pivot	Link length
p_1	(6.97, −7.25)	(7.58, −6.65)	12.96
p_2	(−22.12, −19.56)	(−6.11, 6.08)	31.38
p_3	(−23.14, 14.33)	(−26.71, 12.56)	14.40
p_4	(−53.13, −64.84)	(−1.88, 14.02)	93.25

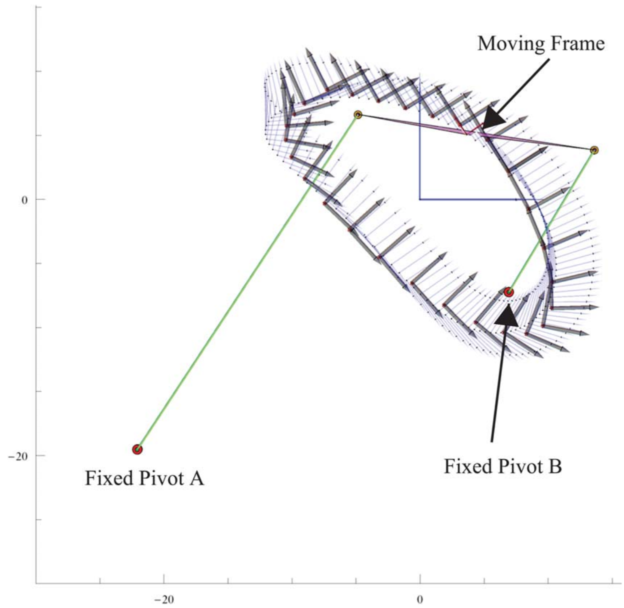

Fig. 5 The one-DOF four-bar upper-limb rehabilitation mechanism designed to approximately lead through the 28 task poses in Fig. 4

platform is designed so that the four-bar linkage could be fixed on. The height and the angle of the platform could be adjusted to suit the users' comfort. Specifically, the height of the device is adjusted by the support bar, the angle of the platform (pitch angle) is adjusted by the connecting joint between the table board and the support bar, and the initial angle of the four-bar linkage (roll angle) is adjusted by the two fixed pivots of the linkage. The structure of this device is shown in Fig. 6.

We use STC12C5A60S2 chip to build and control the rehabilitation system. Also, to measure the contact pressure between the

Fig. 6 Design of the upper-limb rehab device incorporated with the one-DOF motion executer as shown in Fig. 5

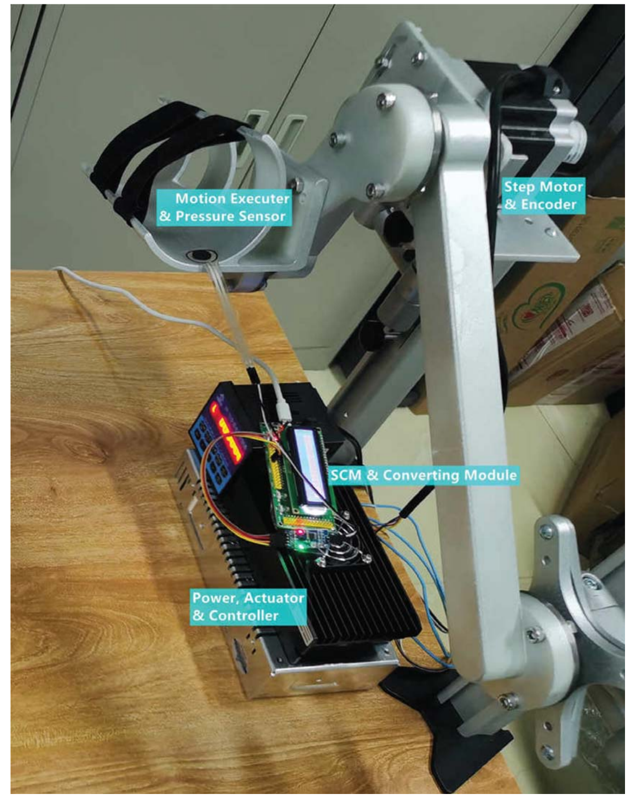

Fig. 7 The actual rehabilitation device

motion executor and patient's upper limb, FSR film pressure sensor is used. The sensor first outputs its voltage U_0 to the SCM through the conversion module, and then, this voltage signal is converted to the measured pressure F to the user interface through the following equation:

$$U_0 = 3.2/F_{\max} \times F + 0.1 \tag{4}$$

where U_0 is the output voltage value from the AO port of FSR pressure sensor, F is the pressure, and $F_{\max}$ is the maximum measurement value of the FSR sensor, which in our system is 6000 g.

To drive the one-DOF motion executor, an 86 cm 45 step motor is used with DY-IS step controller as shown in Fig. 7. MA860C driver and YT06-0P incremental photoelectric rotary encoder are embedded to control and record the speed of rotation. Conversion between the motor speed ω and count pulse of the encoder is expressed as follows:

$$\omega = 2\pi \times N/M \tag{5}$$

where N is the count pulse that received by the SCM from the encoder within unit time and M denotes the line number of the encoder, i.e., the resolution.

4 Design of Immersive Upper-Limb Rehabilitation User Interface Based on Virtual Reality

As stated in Sec. 1, generally the training process involves a large amount of repetition of rehab motion on a daily basis, which could be quite tedious for most patients. Considering the patients' enthusiasm to perform the rehab training could easily drop in plain training, in this section, we adopt VR technique to create an immersive rehabilitation training mode. More specifically, we design a VR-integrated rehabilitation training user interface based on the Unity3D engine. The virtual rehabilitation training system has a real interactive experience, which makes patients feel immersive in training and get positive feedback. This system can provide

Fig. 8 The VR-based user interface for upper-limb rehabilitation training patients

repeated stimulation and entertainment during the training process, and it could also help maintaining the rehab motion that has been practiced.

As shown in Fig. 8, a model of rowing boat is constructed to simulate the immersive environment for the boating motion of the rehabilitation task. In addition, a series of scenes such as hull and lake surface are built using SOLIDWORKS software. The screen is used as the virtual display to reflect and interact with the actual rehab training behavior. After building the three-dimensional model, 3DMAX is adopted to generate an *fbx* file for the streamlining and rendering process. Finally, the *fbx* file was imported into UNITY3D for development of the character features and the boating scene. To reduce the resource occupation during program running, the character features have been simplified, such that the whole arm is reflected in the VR game as a control feature. The speed parameters of the motor are transmitted from the rehabilitation device to the host computer through the USB serial port. The character control script in this VR game reads the speed parameters of the serial port to control the character's arm for rowing motion. Initialization is required at the beginning of the game to match the current position of the rehabilitation mechanism. The mapping relationship between the virtual model and the real device is set as follows:

$$\omega_r = \omega_1 \tag{6}$$

where ω_r denotes the rotation angular velocity of the character's arm in the VR rowing game and ω_1 is the angular velocity of the crank link in the rehabilitation device.

By detecting the pulse frequency of the motor, the speed of the upper-limb movement can be obtained. Through the mapping between actual rehab motion and the virtual model, the transformation of the actual coordinates and the virtual motion coordinates is calculated, and then the spatial coordinates of a group of essential point is acquired and converted into a motion sequence composed of a series of animation frames. Through that, a three-dimensional space motion process is described, and a three-dimensional

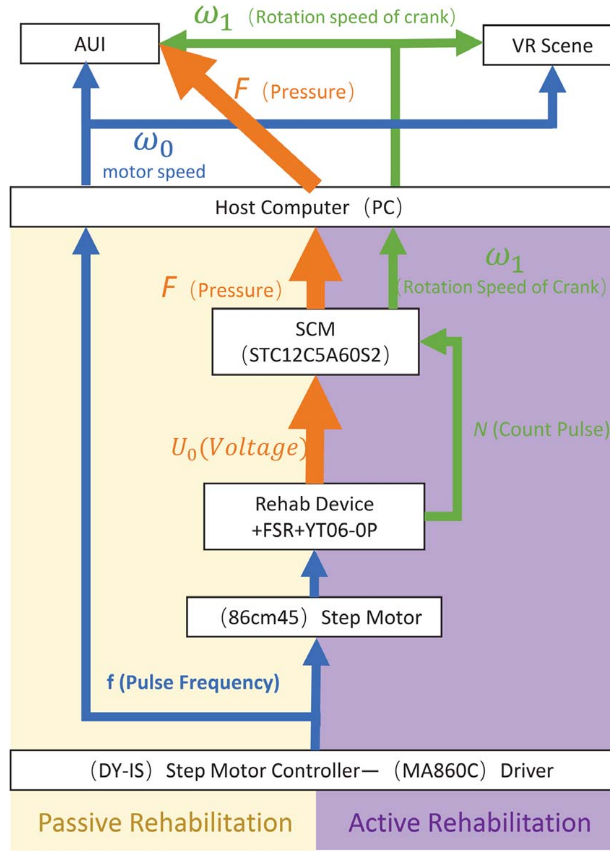

Fig. 10 The two-mode (PR and AR) strategy of the proposed upper-limb rehabilitation system

character skeleton animation source file is then created. This process is shown in Fig. 9.

When the patient starts the training process and the device is set in the initial state, the spatial origin in UNITY3D matches the point transmitted by the hardware driver, so that the arm position in the virtual environment is consistent with the patient's sitting position. During the rehab training motion, the data are obtained and transmitted to the UNITY3D software through the drive interface to generate the virtual movement in the user interface. In the end, the interaction between the patient and the virtual reality not only provides an immersive experience for the rehab training user but could also let the medical caring staff observe the real-time motion effect and record the rehab training data for each patient.

5 Integration and Experiment of the System

In this section, the rehabilitation mechanism as shown in Fig. 7 and the VR-based rehab user interface are combined to construct

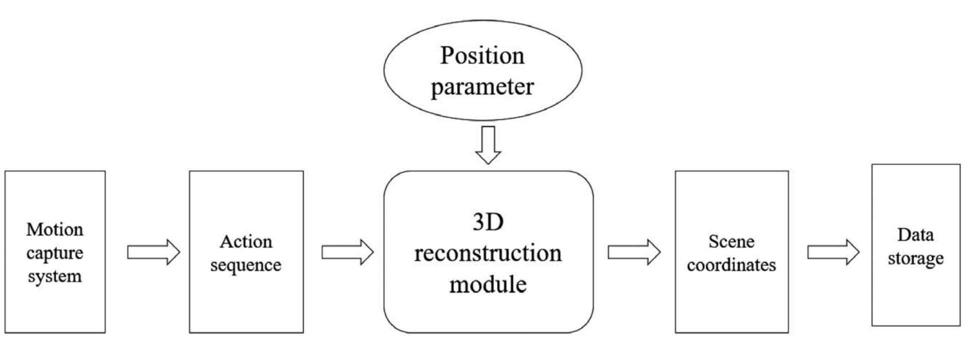

Fig. 9 Implementation process of the VR-integrated rehabilitation approach

(*a*)

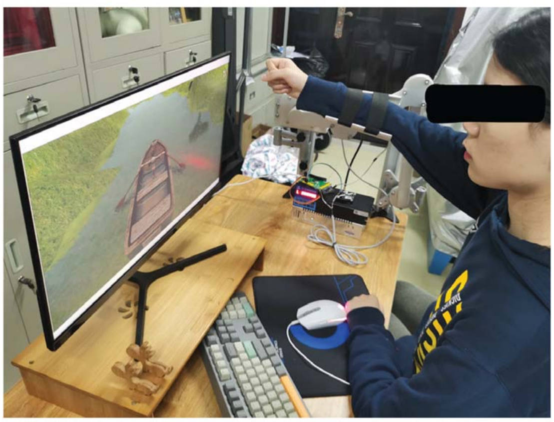

(*b*)

Fig. 11 These two figures show the prototype of the upper-limb rehab device and how it is applied to a user

an immersive upper-limb rehab system. Considering the proceeding of rehab training, to suit patients in different rehab condition, we set two modes in the system: passive rehabilitation and active rehabilitation. In the *passive rehabilitation* mode (PR mode), the operation of the rehab motion executer is only driven by the motor, and the patients' upper-limb motion are completely controlled by the device. During the PR mode, the speed of the motor is controlled variable, which is adjusted according to the initial settings at the start of the rehab training. During the entire training process, the patient's arms are naturally relaxed and is driven by the executer to perform rehabilitation movements according to a predetermined trajectory. Conversely, in the *active rehabilitation* mode (AR mode), a pressure sensor is installed on the arm cover to detect the pressure between patients' upper limb and the motion executer, and the speed of the motion executer is also calculated by the pulse frequency of the motor. These parameters could be recorded so as to reflect the patient's motion performance, and the current training state could then be evaluated.

The two-mode rehabilitation strategy of this system is illustrated in Fig. 10. In the passive rehabilitation mode, the controller sends commands to the driver, and the driver outputs a given pulse to drive the stepping motor to rotate at a certain angular speed. When the rehabilitation device is driven to operate, the pressure sensor starts to measure the pressure between the patient's upper limb and the mechanism. The obtained pressure signal is then obtained and passed to the SCM, which calculates the pressure value and transmits to the host computer through the USB serial port. The pressure value and the motor speed are displayed in real time on the administrator user interface for the caring staff to monitor the status of the patients. At this time, on the patient's user interface, the rowing motion of the character in the VR is driven and controlled by the angular velocity of the motor.

In the active rehabilitation mode, the mechanism is driven by the patients. The pressure sensor and incremental encoder start to record the motion parameters including the pressure between the upper limb and the executor, as well as the angular velocity value of the rowing movement. The pressure is acquired similarly as shown in the PR mode, while the angular velocity is obtained by

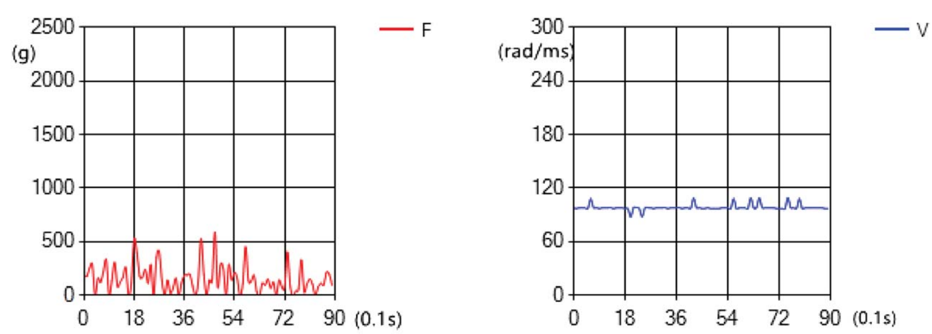

(*a*)

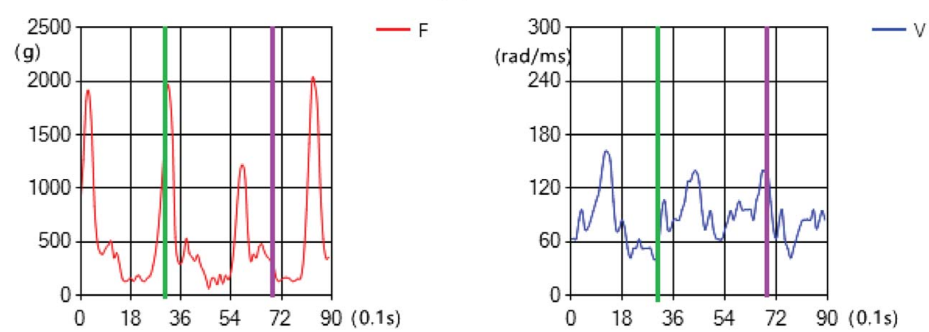

(*b*)

Fig. 12 Real-time diagram of the pressure and angular velocity data of the (*a*) PR and (*b*) AR human trial results

converting the count pulses obtained by the YT06-0P encoder through the SCM.

For both modes, the patients' motion data are captured by the sensor and sent to the VR display system, so that the real-time training performance could be reflected. Also, the training parameters such as the rotational speed, the time of duration, as well as the pressure could all be recorded to help the medical caring staff evaluate the rehab status of patient's upper limb.

The illustration of the prototype of VR-integrated upper-limb rehabilitation system is shown in Fig. 11, as well as how it is applied to a user. A trial of the system on a human subject is also conducted for both PR and AR training modes. The user attaches the forearm to the motion executor with straps to fasten it. The rotational speed is detected by the encoder installed at the end of the step motor, and the pressure sensor is installed close to the end of the elbow on the arm rest, which detects the real-time pressure of the subject's forearm arm. First PR training is conducted by the subject, in which the rehab motion is purely driven by the motor. Figure 12(*a*) shows the real-time diagram of the pressure and angular velocity data. The horizontal axis of the two diagrams denotes the time of training. From the result, we can find that since there is no active control to the subject's forearm, the pressure detected is merely due to the gravity, which shows no obvious periodic variation. Also, during PR training, the motion is driven by the motor; thus, the velocity only reflects the preset motor speed, which basically is a constant value on the diagram.

In the AR training trial, the subject put the forearm on the device and complete the rowing movements independently. The diagram of pressure and speed are also plotted in Fig. 12(*b*), with the same legend and unit as in PR trial. It can be observed that there exist obvious periodic patterns in both pressure and velocity. Moreover, we could further notice that when the subject's elbow moves to the lowest point of the motion, it starts to exert force to raise the forearm, bringing a peak value in the pressure diagram, and meanwhile, the speed diagram reaches a valley, as shown by the green line at 3.0 s of the horizontal axis of the figure. Conversely, when the elbow of the arm is raised to the highest point and ready to fall, the arm muscles are relaxed and the measured pressure value reaches a valley, and the speed diagram generates a peak, as shown by the purple line at 6.9 s of the horizontal axis of the figure.

6 Conclusions

In this article, we presented a VR-integrated upper-limb rehabilitation device with single-DOF. First, the regression motion of the clustering result were taken as the task motion, and kinematic-mapping-based motion synthesis framework was adopted to design the one-DOF four-bar linkage mechanism as the motion executer. Then, an immersive rehab system with UNITY3D based on VR was developed to address the issue of large amounts of repetition in the practical rehab training process, with a two-mode (PR and AR) rehabilitation strategy. This rehabilitation device is simple, low cost, and easy to control, and it could provide the patients with an immersive rehab training experience. Future work includes the improvement of the mechanical structure, as well as the further utilization of the rehab data collected by the system so as to provide a better rehab therapy.

Acknowledgment

The work has been financially supported by National Key R&D Program of China (Ping Zhao; Grant No. 2019YFB1311603), National Natural Science Foundation of China (Ping Zhao; Grant No. 51775155), and Anhui Provincial Key R&D Project (No. 201904b11020035). All findings and results presented in this article are by those of the authors and do not represent the funding agencies.

Conflict of Interest

There are no conflicts of interest.

Appendix: Coordinates for the Elbow and Wrist Trajectories of the Blue Cluster

Index	Elbow	Wrist
1	[−160.12, 44.009, 1071.1]	[−148.86, 190.19, 947.29]
2	[−154.27, 34.923, 1083.0]	[−154.48, 187.71, 982.99]
3	[−158.70, 33.887, 1092.9]	[−159.57, 191.31, 1027.6]
4	[−167.56, 41.237, 1102.1]	[−162.12, 201.02, 1075.3]
5	[−177.38, 55.813, 1111.5]	[−161.14, 217.13, 1125.2]
6	[−186.44, 77.343, 1122.1]	[−155.93, 238.71, 1172.4]
7	[−192.85, 104.09, 1133.8]	[−146.87, 263.78, 1212.8]
8	[−195.66, 133.45, 1145.7]	[−133.93, 292.37, 1246.3]
9	[−194.73, 165.34, 1157.7]	[−118.18, 322.1, 1269.6]
10	[−190.04, 197.0, 1168.7]	[−101.28, 350.31, 1280.9]
11	[−182.37, 225.69, 1177.2]	[−83.503, 376.95, 1280.3]
12	[−172.08, 251.43, 1182.7]	[−66.698, 399.41, 1266.8]
13	[−160.38, 271.69, 1184.2]	[−52.604, 415.75, 1241.9]
14	[−148.74, 284.86, 1180.8]	[−41.495, 425.82, 1205.2]
15	[−137.57, 290.93, 1172.2]	[−34.809, 428.18, 1159.1]
16	[−128.33, 288.92, 1158.2]	[−33.158, 422.74, 1108.0]
17	[−122.07, 279.37, 1139.9]	[−36.564, 409.53, 1052.2]
18	[−119.04, 262.54, 1117.4]	[−44.822, 389.52, 997.6]
19	[−119.80, 240.16, 1092.9]	[−56.543, 365.28, 950.83]
20	[−124.09, 215.41, 1069.8]	[−70.726, 338.04, 915.08]
21	[−124.09, 215.41, 1069.8]	[−70.726, 338.04, 915.08]
22	[−130.33, 193.41, 1051.5]	[−81.442, 318.04, 902.71]
23	[−139.97, 171.41, 1046.6]	[−91.574, 298.04, 887.25]
24	[−146.64, 149.41, 1046.7]	[−103.31, 278.04, 887.62]
25	[−152.75, 127.41, 1047.4]	[−117.50, 258.04, 895.18]
26	[−157.81, 105.41, 1048.8]	[−131.20, 238.04, 905.75]
27	[−161.26, 83.409, 1050.9]	[−141.38, 218.04, 916.53]
28	[−162.55, 61.409, 1054.0]	[−145.47, 198.04, 925.02]

References

[1] Spong, M. W., Hutchinson, S., and Vidyasagar, M., 2006, *Robot Modeling and Control*, Wiley, New York.

[2] D'Onofrio, G., Fiorini, L., Hoshino, H., Matsumori, A., Okabe, Y., Tsukamoto, M., Limosani, R., Vitanza, A., Greco, F., and Greco, A., 2018, "Assistive Robots for Socialization in Elderly People: Results Pertaining to the Needs of the Users," Aging Clin. Exp. Res., **31**(9), pp. 1313–1329.

[3] Sugar, T. G., He, J., Koeneman, E. J., Koeneman, J. B., Herman, R., Huang, H., Schultz, R. S., Herring, D. E., Wanberg, J., and Balasubramanian, S., 2007, "Design and Control of RUPERT: A Device for Robotic Upper Extremity Repetitive Therapy," IEEE Trans. Neural Syst. Rehabil. Eng., **15**(3), pp. 336–346.

[4] Holt, R., Makower, S., Jackson, A., Culmer, P., and Bhakta, B., 2007, "User Involvement in Developing Rehabilitation Robotic Devices an Essential Requirement," Proceedings of IEEE 10th International Conference on Rehabilitation Robotics, The Netherlands, June 12–15, IEEE, pp. 219–227.

[5] Zhang, Y. B., Wang, Z. X., Ji, L. H., and Bi, S., 2005, "The Clinical Application of the Upper Extremity Compound Motions Rehabilitation Training Robot," IEEE International Conference on Rehabilitation Robotics, Chicago, IL, June 28–July 1, IEEE, pp. 91–94.

[6] Perry, J. C., Rosen, J., and Burns, S., 2007, "Upper-Limb Powered Exoskeleton Design," IEEE/ASME Trans. Mechatron., **12**(4), pp. 408–417.

[7] Haraguchi, M., Kikuchi, T., Jin, Y., Fukushima, K., Furusho, J., and Inoue, A., 2007, "3-D/Quasi-3-D Rehabilitation Systems for Upper Limbs Using ER Actuators With High Safety," IEEE International Conference on Robotics and Biomimetics, Sanya, China, Dec. 15–18, IEEE, pp. 1482–1487.

[8] Naghavi, N., and Mahjoob, M. J., 2015, "Design and Control of an Active 1-DoF Mechanism for Knee Rehabilitation," Disabil. Rehabil. Assist. Technol., **2015**(7), pp. 1–7.

[9] Franci, R., Parenti-Castelli, V., Belvedere, C., and Leardini, A., 2009, "A New One-DOF Fully Parallel Mechanism for Modelling Passive Motion at the Human Tibiotalar Joint," J. Biomech., **42**(10), pp. 1403–1408.

[10] Zhao, P., Zhu, L., Li, X., and Zi, B., 2019, "Design of Planar 1-DOF Cam-Linkage for Lower-Limb Rehabilitation Via Kinematic-Mapping Motion Synthesis Framework," ASME. J. Mech. Rob., **11**(4), p. 041006.

[11] Chen, W., Song, W., Chen, H., Li, Q., and Zhao, P., 2019, "Motion Synthesis for Upper-Limb Rehabilitation Motion With Clustering-Based Machine Learning Method," Proceedings of the ASME 2019 International Mechanical Engineering Congress and Exposition. Volume 3: Biomedical and

Biotechnology Engineering, Salt Lake City, UT, Nov. 11–14, ASME, p. V003T04A066.
[12] Erdman, A. G., and Sandor, G. N., 1997, *Mechanism Design: Analysis and Synthesis*, 3rd ed, Prentice Hall, NJ.
[13] Angeles, J., and Bai, S., 2005, "Some Special Cases of The Burmester Problem for Four and Five Poses," 2005 ASME Design Engineering Technical Conferences, Long Beach, CA, Sept. 24–28, Paper No. DETC2005-84871.
[14] Ge, Q. J., Zhao, P., Li, X., and Purwar, A., 2012, "A Novel Apporach to Algebraic Fitting of Constraint Manifolds for Planar 4R Motion Approximation," 2012 ASME Mechanisms and Robotics Conference, Chicago, IL, Aug. 12–15, Paper No. DETC2012-71190.
[15] Zhao, P., Li, X., Zhu, L., Zi, B., and Ge, Q. J., 2016, "A Novel Motion Synthesis Approach With Expandable Solution Space for Planar Linkages Based on Kinematic-Mapping," Mech. Mach. Theory., **105**(11), pp. 164–175.
[16] Zhao, P., Ge, Q. J., and Purwar, A., 2004, "On the Complete Synthesis of Finite Positions With Constraint Decomposition via Kinematic Mapping, ASME 2014 International Design Engineering Technical Conferences and Computers and Information in Engineering Conference, Buffalo, NY, Paper No. V05AT08A052.
[17] Bottema, O., and Roth, B., 1979, *Theoretical Kinematics*, North-Holland, Amsterdam.
[18] McCarthy, J. M., 1990, *Introducation to Theoretical Kinematics*, MIT, Cambridge, MA.
[19] Ravani, B., and Roth, B., 1983, "Motion Synthesis Using Kinematic Mappings," ASME J. Mech., Transm., Autom. Des., **105**(3), pp. 460–467.
[20] Bodduluri, R., and McCarthy, J. M., 1992, "Finite Position Synthesis Using the Image NCurve of a Spherical Four-Bar Motion," ASME J. Mech. Des., **114**(1), pp. 55–60.
[21] Ge, Q. J., and Larchelle, P., 1999, "Algebraic Motion Approximation With NURBS Motions and Its Application to Spherical Mechanism Synthesis," ASME J. Mech. Des., **121**(4), pp. 529–532.
[22] Wu, J., 2010, "Interactive Dimensional Synthesis and Motion Design of Planar 6R Single-Loop Closed Chains Via Constraint Manifold Modification," ASME. J. Mech. Rob., **2**(3), p. 031012.
[23] Hayes, M. J. D, and Rusu, S. R., 2011, "Quadric Surface Fitting Applications to Approximate Dimensional Synthesis," 13th World Congress in Mechanism and Machine Science., Guanajuato, Mexico, June 19–25.
[24] Li, X., Ge, X., Purwar, A., and Ge, Q. J., 2015, "A Unified Algorithm for Analysis and Simulation of Planar Four-Bar Motions Defined With R- and P-Joints," ASME. J. Mech. Rob., **7**(1), p. 011014.
[25] Veerbeek, J. M., van Wegen, E., van Peppen, R., van der Wees, P. J., Hendriks, E., Rietberg, M., and Kwakkel, G., 2014, "What Is the Evidence for Physical Therapy Poststroke? A Systematic Review and Meta-Analysis," PLoS One., **9**(2), p. e87987.
[26] Y. Park, C.-H. Morone, and B. -H. Lee, 2013, "Clinical Usefulness of the Virtual Reality-Based Postural Control Training on the Gait Ability in Patients With Stroke," J. Exercise Rehabilitation, **9**(5), pp. 489–494.
[27] Morone, G., Tramontano, M., Iosa, M., Shofany, J., Iemma, A., Musicco, M., Paolucci, S., and Caltagirone, C., 2014, "The Efficacy of Balance Training With Video Game-Based Therapy in SubAcute Stroke Patients: A Randomized Controlled Trial," BioMed. Res. Int., **2014**, p. 580861.
[28] Rose, T., Nam, C. S., and Chen, K. B., 2018, "Immersion of Virtual Reality for Rehabilitation - Review," Appl. Ergon., **69**(2018), pp. 153–161.
[29] Standen, P. J., Threapleton, K., Richardson, A., Connell, L., Brown, D. J., Battersby, S., Platts, F., and Burton, A., 2017, "A Low Cost Virtual Reality System for Home Based Rehabilitation of the Arm Following Stroke: A Randomised Controlled Feasibility Trial," Clinical Rehabil., **31**(3), pp. 340–350.